GMR
The Original

SUSTAINED ANTIMICROBIAL URETERAL STENT COATING USING A *WITHANIA SOMNIFERA*-SILVER NANOCOMPOSITE: AN IN VITRO EVALUATION OF ANTIBIOFILM ACTIVITY AND DURABILITY

Manshad CK[1], B David Jayseelan[2]

[1,2]Department of Microbiology, Nehru College of Arts and Science, Coimbatore, India

ABSTRACT:
The present study aimed to evaluate antibacterial coatings for ureteral stents to prevent urinary tract infections associated with stent indwelling. Withania somnifera and silver nanoparticles were developed as a novel composite and coated onto stent materials under laboratory conditions. The coated stents were characterized using field emission scanning electron microscopy (FESEM); to evaluate the antibacterial activity qualitatively and quantitatively; to measure the anti-biofilm activity and to investigate the durability in terms of antibacterial activity. The coated stents on the qualitative assay demonstrated visible inhibitory zones confirming antimicrobial activity against clinical strains. In addition, quantitative analysis demonstrated a statistically significant ($P < 0.05$) reduction in the number of bacteria attached to the coated stent surfaces. No bacterial colonization was observed on the coated stents, even after the second challenge cycle (72 h), no challenge isolates were found on surface of coated stents as assessed by an in vitro challenge test. The in-vitro analysis of this system, which also demonstrated effective biocompatibility and favourable degradation characteristics of the in vitro analysis also demonstrated favourable degradation behaviour and controlled drug release characteristics suitable for antimicrobial ureteral stent applications combined with controlled drug release highlights some key requirements for future anti-infective ureteral stents. This approach enables the generation of high local drug concentrations at the target site while minimizing systemic exposure and the complete suppression of physiological bacterial proliferation through continual local release.

KEYWORDS: Ureteral stents; Nanoparticles; Anti-biofilm; In vitro challenge; Composite

INTRODUCTION

A ureteral stent is used in urology to ensure that urine can exit the kidney and also to keep the ureter open. (Brotherhood et al., 2014) Ureteral stents are commonly used in the medical community. At the same time, associated stents often lead to complications like encrustation and biofilm formation on the device surface or urinary disease infections (Kehinde et al., 2004). Consequently, bacterial persistence and antimicrobial resistance may increase.

Once established, biofilms provide a protective niche for living organisms, allowing microorganisms to survive antimicrobial treatment and host defense mechanisms(Zelichenko et al., 2013).

Adhesion of bacteria to a biofilm on the stent surface is the first step in stent-associated infection, followed by the production of an extracellular polymeric matrix that facilitates biofilm development to build up that biofilm architecture. (Zelichenko et al., 2013) Commonly implicated uropathogens infecting stents include *Escherichia coli*, *Staphylococcus aureus*, *Pseudomonas aeruginosa, Enterococcus species*. (Liaw and Knudsen, 2016) Sustained high pressures in the ureter and kidney can cause infection even if the stent has been utilized in the very short term (Scotland et al., 2019).

Prophylactic antibiotics are recommended before stent placement and have limited effectiveness in preventing biofilm-associated bacterial growth or antimicrobial resistance trends overall. (Kehinde et al., 2004)

To combat these issues with urological stents, surface modification strategies targetingmicrobial adhesion prevention have attracted increasing attention. Antimicrobial coatings providing persistent and local drug release represent an appealing avenue of research to diminish device–tissue interactions. Nanotechnology has shown that silver nanoparticles (Ag NPs) and other novel materials provide broad-spectrum antibacterial action via various mechanisms, including membrane disruption leading to organelles' malfunction; interference with protein synthesis and even halting nucleic acid replication. (Silva et al., 2009) Meanwhile, as alternative antimicrobial agents, plant-derived bioactive compounds attract attention because of their excellent biocompatibility and rich array of active chemicals. This traditional medicine herb, *Withania somnifera* (L.) Dunal, has been found to have antimicrobial effects and can prevent biofilm formation. (Owais et al., 2005; Mathur et al., 2007; Ansari et al.,

2025) Mixtures of plant extracts with metal nanoparticles could produce mutually reinforcing antimicrobial effects by combining the actions of plant compounds with nanoparticle-mediated bacteria killing. (Vazquez-Munoz et al., 2019). The aims of this study were to develop a novel herbal–metal composite (HMc) composed of *Withania somnifera* extract and silver nanoparticles as a coating material for ureteral stents, and to assess its antimicrobial properties, anti-biofilm efficacy, and durability under surface-attached in vitro conditions.

MATERIALS AND METHODS

The experiments were conducted in the Department of Microbiology, Nehru College of Arts and Science, Coimbatore, India., Nehru College of Arts and Science, Coimbatore, India. Clinical strains of E*scherichia coli* and *Staphylococcus aureus* were selected as prototype Gram-negative and Gram-positive organisms respectively. Fresh leaves of *Withania somnifera* were obtained locally and authenticated prior to extraction. Commercial ureteral stents (6 Fr, 26 cm; INDOVASIVE, Biorad Medisys Pvt. Ltd. (Pune, India) was used as the base material for coating.

Preparation of *Withania somnifera* Extract

The leaves were washed, shade-dried, and subsequently dried in an oven at 40°C until the moisture content was below 10%. The dried material was crushed and screened (250 µm). The extraction in methanol on Soxhlet apparatus was done for 6 hours with controlled temperature. Further the extract was concentrated at 40-50 °C (Pooja Dhama et al., 2023).

Synthesis of Silver Nanoparticles

Silver nanoparticles were synthesized using a chemical reduction method. In short, a 0.01 M silver nitrate solution was warmed until boiling and then 1% (w/v) trisodium citrate was dropped into it under continuous stirring. The formation of silver nanoparticles was visually confirmed by a colour shift (from pale yellow to brown). The liquids were further stirred at 80-90°C for 25 min then centrifuged at 6500 rpm, 25 min), washed with distilled water five times, and oven-dried. Further, liquid suspensions were characterized by UV–Vis spectroscopy, particle size analysis, zeta potential measurement, X-ray diffraction and SEM analysis (Kiran Kedar et al., 2022).

Minimum Inhibitory Concentration (MIC) Assay Test

Antimicrobial activity of W. somnifera extract and silver nanoparticles were analysed by the agar well diffusion method (Ansari et al., 2025; Kakian et al., 2024). The bacterial suspensions were set to 0.5 McFarland standard and inoculated on Mueller–Hinton agar plates. Concentrations of extracts between 100–500 µg/mL and nanoparticles between 10–50 µg/mL were tested. After which, plates were incubated at 37°C for 24 h and inhibition zones measured. MIC was developed as the least fixed concentration showing a visible inhibition zone.

Preparation of Herbal–Metal Composite (HMc)

The silver nanoparticle suspension was mixed with W. somnifera extract under continuous magnetic stirring (180 rpm, 40°C) and the herbal–metal composite was prepared. The extract was then added dropwise (1 mL/min) and stirred for 2 h to ensure homogeneous composite formation. This solution was transferred and stored in sterile amber containers at 4 °C (Meenakshi and Kalai Gandhi, 2016).

Coating of Ureteral Stents

The stents (10 mm length) were dip-coated. A slurry was prepared of herbal–metal composite with polyethylene glycol (PEG) and kept homogenized at 40–45°C; stents were immersed in the suspension for 30 Min (120 rpm), air-dried, recoated to ensure homogenous coverage. A secondary tocopherol acetate layer (10% w/w in DMSO) was deposited by cycles of brief immersion with PBS rinsing to control drug release and provide coating stability. Freeze–thaw conditioning was performed to obtain physical crosslinking (Lenzuni et al., 2024).

FESEM Surface Characterization

Field Emission Scanning Electron Microscopy (FESEM) was used to identify surface morphology of coated and uncoated stents. 6000× EM images were taken to evaluate coating uniformity and surface topography.

Anti-Biofilm Activity (MBEC Determination)

The ability to eliminate biofilms was studied by modified microdilution method (Perumal and Mahmud, 2013). Bacterial suspensions (1 × 106 CFU/mL) was added to 96 wells microtiter plates and incubated for 24 h for biofilm formation. Subsequently, after washing with PBS, serial dilutions of herbal extract, silver nanoparticles and composite were added. After incubation, the lowest concentration that prevented visible growth of biofilm was termed MBEC. Experiments were performed in triplicate.

Qualitative Antibacterial Evaluation of Coated Stents

Agar diffusion assay was performed to test the antimicrobial activity of coated stents. Stent segments with predefined measurements were deposited on Mueller–Hinton agar plates previously seeded with test organism for 24h at 37°C and the resulting inhibition zones measured and compared to uncoated controls (Lenzuni et al., 2024).

Quantitative Bacterial Adherence Assay
The adherence of bacteria was analyzed through an artificial urine medium created as previously mentioned (Multanen, 2002). Stent segments coated and uncoated were incubated with bacterial suspensions (2.5×10^5 CFU/mL) for 3 h at the gentle agitation. The stents were resuspended in sterile PBS and sonicated to recover adhered bacteria. The number of colony-forming units (CFU) was assessed by serial dilution plating. Results are reported as ratio of detached bacteria to inoculum dose. The remaining planktonic bacteria were also counted.

Statistical Analysis
Chi-square analysis were used to assess statistical significance, with $P < 0.05$ being considered significant.
Antimicrobial durability (In vitro Assessment)
Antimicrobial durability was evaluated through sequential active bacterial tests of stents coated with the herbal–metal composite. The stents were then immersed in nutrient broth containing either *E. coli* or *S. aureus* and incubated at 37°C with shaking at 80 rpm. Turbidity was monitored daily using media. After 7 days of no colonization, a second challenge dose was given. Resistance to colonization was measured through repeated cycles of exposure.

RESULTS AND DISCUSSION
Herbal Extracts and Minimal inhibitory concentration
The minimal inhibitory concentration (MIC) of *Withania somnifera* extract against *Escherichia coli* and *Staphylococcus aureus* was determined by standard agar well diffusion method for various solvent extracts. An inhibitor effect for each solvent and different concentrations have been provided in Table-2.

Table-2: Minimal inhibitory concentration (MIC) of *Withania somnifera*

Extract Type	Bacterial Strain	100 µg/mL	200 µg/mL	300 µg/mL	400 µg/mL	500 µg/mL
Methanolic	*E. coli* (B1)	–	–	13.3 ± 1.05	17.6 ± 0.75	20.3 ± 1.05
	S. aureus (B2)	–	–	8.6 ± 0.75	12.3 ± 1.05	15.9 ± 0.57
Ethanolic	*E. coli* (B1)	–	–	11.6 ± 0.75	14.6 ± 0.75	18.3 ± 1.05
	S. aureus (B2)	–	–	10.9 ± 0.12	16.3 ± 1.05	17.6 ± 0.75
Acetone	*E. coli* (B1)	–	–	11.3 ± 1.05	13.9 ± 0.57	18.3 ± 1.05
	S. aureus (B2)	–	–	9.6 ± 0.75	12.9 ± 0.57	17.3 ± 1.05
Petroleum Ether	*E. coli* (B1)	–	–	–	13.9 ± 0.57	17.6 ± 0.75
	S. aureus (B2)	–	–	10.6 ± 0.75	12.3 ± 1.05	18.6 ± 0.75
Aqueous	*E. coli* (B1)	–	–	–	11.9 ± 0.57	14.3 ± 1.05
	S. aureus (B2)	–	–	7.9 ± 0.57	7.6 ± 0.75	12.6 ± 0.75

The antibacterial activity of various solvent extracts of *Withania somnifera* against *Escherichia coli* and *Staphylococcus aureus* is shown in table 2 and figure 2. All extracts exhibited a concentration-dependent inhibitory effect against both test organisms. At lower concentrations (100 µg/mL and 200 µg/mL) No measurable antibacterial activity was observed at concentrations of 100 or 200 µg/mL for any extract tested. Inhibition zones became detectable at concentrations ≥300 µg/mL. The methanolic extract showed relatively stronger antibacterial activity than other tested solvents. The inhibition zone against *E.coli* was 13.3 ± 1.05 mm (300 µg/mL) and 17.6 ± 0.75 mm (400 µg/mL), respectively; the corresponding values for *S. aureus* were 8.6 ± 0.75 mm and 12.3 ± 1.05 mm, respectively (Table II). 500 µg/mL was the concentration that showed the maximum inhibition in *E. coli* (20.3 ± 1.05 mm) and *S. aureus* (15.9 ± 0.57 mm); however, differences of zone diameters among concentrations were significant for comparison between the organisms as well, $p < 0.001$ (Table 2). The MIC of the methanolic extract, determined from these results, was found to be 300 µg/mL for both organisms.

MIC values of ethanolic and acetone extracts were similar (300 µg/mL), but the inhibition zones were smaller. The MIC of petroleum ether extract against *E. coli* and *S. aureus* was 400 µg/mL and 300 µg/mL, respectively. However, the MIC of the aqueous extract was relatively higher at 400 µg/mL for *E. coli* and 300 µg/mL for S. aureus, resulting in smaller inhibition zones compared to MeOH (Table I).

Comparison to the different solvent extracts, difference in antibacterial activity can probably be merited due to solubility and extraction efficiency of phytochemicals. Methanol is an organic solvent capable of extracting a wider range of polar and less polar bioactive molecules, such as alkaloids, flavonoids, and phenolic components that are generally attributed to antimicrobial activity. The higher activity exhibited by the methanolic extract indicates that these compounds play an important role in bacterial inhibition in bacterial inhibition (Owais et al., 2005; Mathur et al., 2007; Ansari et al., 2025).

Phytochemicals derived from W. somnifera may exert antibacterial effects through membrane disruption, enzyme inhibition, and interference with cellular metabolic pathways.
Notably, for some of the tested agents, *E. coli* showed slightly bigger inhibition zones than *S. aureus* which indicate that the Gram-negative bacteria are more susceptible than the Gram-positive ones to different antimicrobials. Such variation could be due to differences in cell wall architecture and permeability. The maintenance of relatively higher concentrations compared to silver nanoparticles needed for inhibition is justified as incorporation into a composite system could increase overall antimicrobial effect via synergisms. The moderate and consistent antibacterial activity exhibited by W. somnifera confirms its proficiency as a bioactive species in formulating the herbal–metal composite coating.

Minimal inhibitory concentration of Silver nanoparticles
The antibacterial activity of silver nanoparticles (AgNPs) against *Escherichia coli* and *Staphylococcus aureus* bacteria was determined using the agar well diffusion method, as shown in Table 3 and Figure 3. A concentration dependent increase in antibacterial activity was clearly demonstrated in the data. For both the test organisms, inhibition zones were not measurable at lower concentrations (10 µg/mL, 20 µg/mL). Nevertheless, antimicrobial activity was observed starting from the concentration of 30 µg/mL, where both *E. coli* (17.3 ± 1.05 mm) and *S. aureus* (17.9 ± 0:57 mm) inhibition zones were measured indicative of positive bacteria inhibition zone activity with respect to no inhibition at lower concentrations. The dialysis zone diameter increased progressively with the concentration of nanoparticles. Enhancement of antibacterial activity was observed for moderate concentrations at 40 µg/mL, where at the highest concentration tested (50 µg/mL), larger inhibition zones were produced-20.6 ± 0.75 mm for *E. coli* and 22.3 ± 1.05 mm for S. aureus. Accordingly, MIC of silver nanoparticles for both organism was found to be 30 µg/mL. The concentration-dependent antibacterial activity of silver nanoparticles observed in this investigation supports previously described mechanisms by which AgNP inhibit the growth of microorganisms. Silver nanoparticles have a bactericidal action through multiple mechanisms including the damage of the microorganism membrane, generation of reactive oxygen species, interaction with proteins' thiol groups and deoxyribonucleic acid (DNA) synthesis inhibition (Yaqoob et al., 2020; Vazquez-Munoz et al., 2019; Salman et al., 2023). Non-inhibitory lower concentrations perhaps indicate that the criticial structural damage or oxidative stress which normally occurs while nanoparticles penetrate bacterial cells was not reached due to a comparatively low nanoparticle density.
Promisingly, similar susceptibility patterns were exhibited by both Gram-negative and Gram-positive bacteria (*E. coli* vs. S. aureus), suggesting promising broad spectrum antimicrobial activity. Gram-negative bacteria have an outer membrane, that can reduce the penetration of antimicrobials; however, the nanoscale diameters of AgNPs allow interaction with outer membrane components, allowing for enhanced permeability and intracellular access. The multi-targeted mechanism of action of silver nanoparticles provides significant potential for reducing the likelihood of bacterial resistance development.

Table-3: Minimal inhibitory concentration of Silver nanoparticles

Concentration (µg/mL)	*E. coli*	S. aureus
10–20	No detectable inhibition	---
30	17.3 ± 1.05	17.9 ± 0.57
40	17.9 ± 0.57	18.6 ± 0.75
50	20.6 ± 0.75	22.3 ± 1.05

FESEM analysis - Topographical analysis of coated Stents
herbal–metal composite–coated ureteral stents. The coated samples showed evidential crystalline deposits are evenly dispersed on the entire stent surface, confirming proper deposition of the composite material. The coating was consistent, homogeneous and well-adhered to form a compact layer on the stent substrate. In contrast to uncoated stents, which exhibited surface roughness and micro-depressions, the composite-coated stents exhibited a smoother and even more uniform topography. The solidification of the herbal–metal composite at these layers also would end up decreasing surface roughness and avoiding depressions on the surfaces. This apparent uniform coverage may restrict how many sites are available for bacterial attachment and the resulting biofilm. Uncoated (Figure 4A) and composite-coated (Figure 4B) show morphologies of the stents before coating showing that the surface was not covered compared to after the composite coat where much coverage is seen.

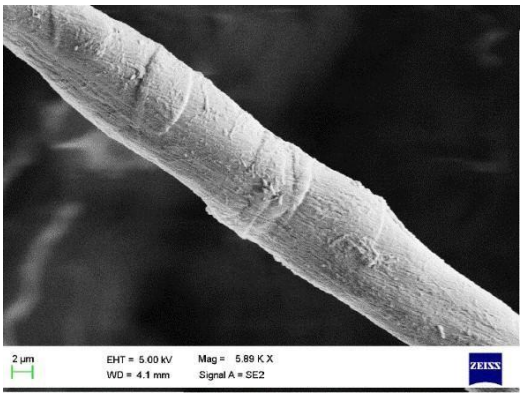

Fig. 4: FESEM analysis - Topographical analysis of coated Stents Fig. 4A: Uncoated ureteral stents

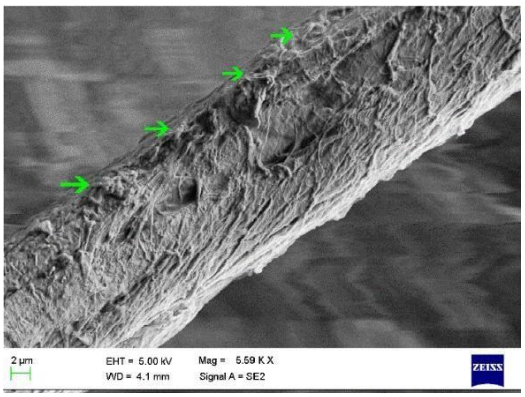

Fig. 4B: Herbal + Metal composite coated ureteral stents

MBEC Analysis of Herbal Extract, Silver Nanoparticles, and Composite Formulation

The anti-biofilm activity of the herbal extract, silver nanoparticles and their herbal–metal composite was evaluated separately using a microdilution-based MBEC assay. The serial concentrations used were from 0.01mg/mL and higher doses tested and summarized in Table 4. The herbal extract exhibited moderate anti-biofilm activity, with MBEC values of 0.25 ± 0.05 mg/mL toward *Escherichia coli* and *Staphylococcus aureus*.

The efficacies of the extract have been enhanced with the application of silver nanoparticles which showed MBEC values to be 0.12 ± 0.05 mg/mL for *E. coli* while it was recorded as 0.25 ± 0.05 mg/mL for S. aureus.

Particularly, the herbal–metal composite showed much improved anti-biofilm effects when compared to single component. *E. coli* MBEC values were 0.06 ± 0.05 mg/mL and *S. aureus* MBEC values were 0.12 ± 0.05 mg/mL for the composite, demonstrating high biofilm eradication abilities in comparison to other antibiofilm agents. These results indicate that biofilm formation is potently inhibited by the composite formulation at concentrations significantly lower than those required for either herbal extract or silver nanoparticles alone.

The biofilm formation on ureteral stents is the most important factor in persistent infections and antimicrobial resistance (Zelichenko et al., 2013; Scotland et al., 2019). Once biofilm is established it helps to shield the bacteria by providing structural protection that decreases antibiotic penetration and increases survival in hostile environment. As such, agents that are effective at preventing or disrupting biofilm formation are of great clinical interest.

The higher anti-biofilm activity of the herbal–metal composite in this study indicates a synergistic effect between phytochemicals from *Withania somnifera* and silver nanoparticles (Yaqoob et al., 2020; Vazquez-Munoz et al., 2019). Phytoconstituents originating from the plant W. somnifera, on the other hand, have also been reported to combat pathogenic bacteria by mediating quorum sensing and biofilm regulatory pathways (Owais et al., 2005; Ansari et al., 2025).

Table 4. Comparative MBEC Values of Individual and Composite Treatments Against Biofilm-Forming Bacteria

Treatment Modality	*E. coli* (mg/mL)	*S. aureus* (mg/mL)
Herbal fraction	0.25 ± 0.05	0.25 ± 0.05
Silver nanoparticles	0.12 ± 0.05	0.25 ± 0.05
Herbal–silver composite	0.06 ± 0.05	0.12 ± 0.05

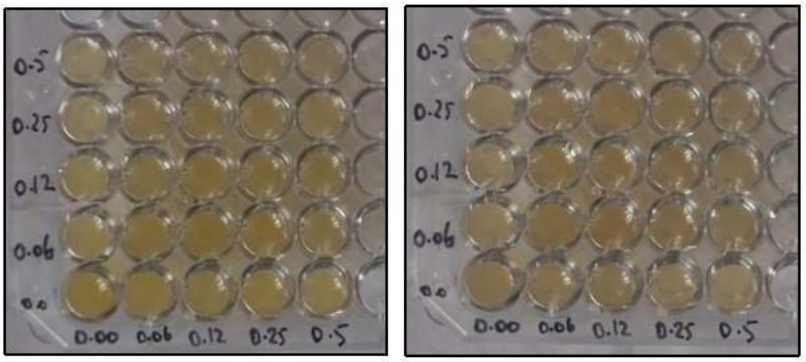

Escherichia coli *Staphylococcus aureus*

Fig. 5: Anti-biofilm activity of herbal + metal composites

Antibacterial activity of coated stents: a qualitative analysis

The antimicrobial activity of the herbal + metal composite coated stents was examined by evaluating the area of inhibition for test bacteria seeded on MHA plate and further calculated as the diffusing ability of drug from implanted stents. In Table-5 and Fig. 6 the clear inhibition zone was observed and measured in mm. All values were statistically calculated after mean and standard deviations. The inhibitory zone size was found to be approximately 26.6 ± 0.75mm against *Escherichia coli* and 24.9 ± 0.57mm against *Staphylococcus aureus* for the composite coated stents respectively

Table-5: Qualitative antibacterial activity of coated stents

Test cultures	Zone of inhibition (in mm)	
	C	UC
Escherichia coli	26.6 ± 0.75	0
Staphylococcus aureus	24.9 ± 0.57	0

C – Herbal + Metal composite coated stents, UC – Uncoated stent

Escherichia coli *Staphylococcus aureus*

C – Herbal + Metal composite coated stents, UC – Uncoated stents

Fig. 6 – Agar diffusion test showing zone of inhibition for test cultures

Quantitative antibacterial activity of coated stents

Quantitative bacterial adherence analysis was carried out using *Escherichia coli* and *Staphylococcus aureus* to assess the anti-adhesive efficiency of the herbal–metal composite coating. Under controlled in vitro conditions, composite-coated stent segments and uncoated stent segments were incubated with standardized bacterial

suspensions. To obtain a quantification of the degree of bacterial adherence, we divided the number of CFU recovered from detached surface-associated bacteria by the initial inoculum dose. Herbal–metal composite–coated stents showed a significantly lower number of surface-adhered bacteria compared with uncoated controls ($P < 0.05$). Despite the variation in CFU between the detached bacteria and inoculum dose which was statistically significantly lower, both organisms exhibited a marked inhibition of early bacterial attachment on coated stents. In comparison, stents lacking a coating displayed significantly elevated levels of adhesion (indicative of microbial susceptibility).

To provide additional information on short-term bacteriostatic or bactericidal activity of agents, residual planktonic bacteria remaining after the incubation period were quantified. The ratio of viable remaining bacterial.

CFU over the original inoculum dose indicated a significant suppression of the bacterial growth in composite-coated stents ($P < 0.05$). Similar effects were observed consistently for both *E. coli* and S. aureus. In contrast, there was no statistically significant reduction in bacterial growth during the incubation period on uncoated stents. Statistical analysis was conducted by the chi-square test, and significant differences were confirmed at $P < 0.05$ (Tables 6 and 7A).

Bacterial attachment to biomaterial surfaces is the first and most crucial event in forming biofilms on indwelling medical devices (Zelichenko et al., 2013; Scotland et al., 2019). When adhesion occurs, microorganisms grow and synthesize extracellular polymeric substances (EPS), allowing for the development of mature biofilms that increase resistance to antimicrobial treatment. Strategies targeting early-stage attachment thus become critical for preventing device-associated infections. The substantial reduction in bacterial adherence observed in this study indicates that the herbal-metal coating effectively modifies the stent surface, thereby limiting bacterial attachment. Silver nanoparticles can damage bacterial membranes and induce oxidative stress, thereby reducing bacterial viability (Yaqoob et al., 2020; Vazquez-Munoz et al., 2019; Salman et al., 2023). Development Of Antimicrobial Phytochemicals: Phytochemicals from *Withania somnifera* have been shown to disrupt the mechanisms responsible for bacterial metabolism and biofilm formation pathways (Owais et al., 2005; Ansari et al., 2025). The synergistic interaction between silver nanoparticles and plant-derived phytochemicals likely enhances the overall antimicrobial efficacy of the coating.

Moreover, the coated stents showed significant inhibition of bacterial growth within this incubation period while reducing adhesion. This suggests that the composite not only prevents initial adhesion but also exhibits prolonged antimicrobial activity that can inhibit residual bacterial populations. Similar results were obtained with other antimicrobial coating systems developed for ureteral stents and urinary implants (Lenzuni et al., 2024; Szell et al., 2019). The ineffectiveness of uncoated stents to limit bacterial attachment and growth agrees with studies reporting that high colonization rates can occur on standard ureteral biomaterials (Kehinde et al., 2004; Rebl et al., 2020). These results strongly support the idea that surface-modification strategies are thus fundamental to preventing stent-associated urinary tract infections.

Table 6. Effect of Phyto–Metal Composite Coating on Bacterial Colonization of Stent Surfaces

Treatment Type	Bacterial Species	Inoculum ($\times 10^3$ CFU)	Surface-Recovered Cells ($\times 10^3$ CFU)	Planktonic Cells ($\times 10^3$ CFU)	p-value
Composite- coated	*S. aureus*	110	7	27	< 0.05
Composite- coated	*E. coli*	124	6	24	< 0.05
Uncoated control	*S. aureus*	110	52	114	< 0.05
Uncoated control	*E. coli*	124	49	121	< 0.05

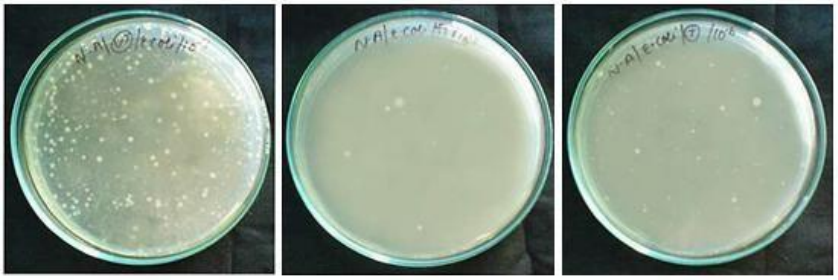

A **B** **C**

A - ID-Inoculum dose, B - DB-detached bacteria, C - RB-Remaining bacteria

Fig. 7A: Viable counts of adhered *Escherichia coli* on coated and uncoated stents

A B C

A - ID-Inoculum dose, B - DB-detached bacteria, C - RB-Remaining bacteria

Fig. 7B: Viable counts of adhered *Staphylococcus aureus* on coated stents

Durability of antibacterial activity on herbal + metal composite applied stents

In vitro challenge assay Results are presented in table 7. For the evaluation, both composite-coated and uncoated stents were tested in triplicates with two bacterial challenge isolates (*Escherichia coli* and *Staphylococcus aureus*). Stents coated with herbal–metal composite exhibited persistent inhibition of bacterial colonization, in the absence of any detectable growth after two challenge cycles for each organism. In contrast, there was clear indication of colonization on uncoated devices after the exposure to test isolates, indicating that these surfaces have no-inherent antimicrobial protection.

Synergistic activity that was established between *Withania somnifera* phytoconstituents and silver nanoparticles results in sustained antimicrobial activity shown by composite-coated stents. Silver nanoparticles are utilized for its bactericidal effects via different mechanisms including disruption of membrane, denaturation of proteins and interference with nucleic acid synthesis (Yaqoob et al., 2020; Vazquez-Munoz et al., 2019; Salman et al., 2023). It is suggested that the first step in stent-associated infection development process is an initial bacterial adhesion (Zelichenko et al., 2013; Scotland et al., 2019). After colonization, biofilm maturation allows for much greater resistance to antimicrobial agents. This unique ability of the composite coating to withstand repeated bacterial challenges indicates its effective inhibition of biofilm establishment at an early adhesion stage. Such attempts with surface-modification strategies have revealed that long-lasting anti-infective coatings are effective in decreasing device-related infections for urological implants (Lenzuni et al., 2024; Szell et al., 2019).

Table 7. Durability of Antimicrobial Coating Under Sequential Bacterial Exposure

Treatment	*E. coli* (Cycle 1 / Cycle 2)	*S. aureus* (Cycle 1 / Cycle2)	Replicates
Composite-coated stent	No colonization / Nocolonization	No colonization / No colonization	3
Bare stent (control)	Colonization / Colonization	Colonization / Colonization	3

CONCLUSION

In this study, a tocopherol acetate-based polymeric coating incorporating a herbal-metal composite of *Withania somnifera* extract and silver nanoparticles was successfully developed for ureteral stent surface modification. The coating functioned as a localized drug-delivery system, enabling sustained release of antimicrobial agents at the implant site while minimizing systemic exposure. Composite-coated stents demonstrated significant antibacterial, antibiofilm, and anti-adhesive properties against urinary tract pathogens under in vitro conditions. Furthermore, the coating exhibited sustained antimicrobial durability during repeated bacterial challenge assays. The synergistic interaction between plant-derived bioactive compounds and silver nanoparticles enhanced antimicrobial performance while maintaining coating stability. Although the findings are limited to in vitro investigations, the results suggest considerable potential for clinical application. Following appropriate in vivo validation, this coating strategy may provide an effective approach for reducing ureteral stent-associated urinary tract infections and improving patient outcomes.

REFERENCES

1. Ansari, F. A., Husain, F. M., Pichtel, J., Meena, R. P., Khan, M. H., Khan, A. S., & Alam, N. (2025). *Withania somnifera* (L.) Dunal: A medicinally important plant inhibits pathogenic biofilms. The Microbe, 6, 100227.
2. Brotherhood, H., Lange, D., & Chew, B. H. (2014). Advances in ureteral stents. Translational Andrology and Urology, 3(4), 314–319. https://doi.org/10.3978/j.issn.2223-4683.2014.06.06
3. Kakian, F., Mirzaei, E., Moattari, A., Shahidi Bonjar, G. H., & Ghasemi, Y. (2024). Determining the cytotoxicity of the minimum inhibitory concentration of silver and zinc oxide nanoparticles in ESBL and carbapenemase-producing Proteus mirabilis. BMC Research Notes, 17, 40.
4. Kehinde, E. O., Rotimi, V. O., Al-Hunayan, A., Abdul-Halim, H., Boland, F., & Al-Awadi, K.

5. A. (2004). Bacteriology of urinary tract infection associated with indwelling J ureteral stents.
6. Journal of Endourology, 18(9), 891–896.
7. Kedar, K., Nayak, S., & Bhaskar, V. H. (2022). Synthesis of silver nanoparticles by chemical reduction method. International Journal of Pharmaceutical Research, 25(3), 364–376.
8. Lenzuni, M., Fiorentini, F., Summa, M., Bertorelli, R., Suarato, G., Perotto, G., & Athanassiou,
9. A. (2024). Electrosprayed zein nanoparticles as antibacterial and anti-thrombotic coatings for ureteral stents. International Journal of Biological Macromolecules, 257, 128560.
10. Liaw, A., & Knudsen, B. (2016). Urinary tract infections associated with ureteral stents: A review. Archivos Españoles de Urología, 69(8), 479–484.
11. Mathur, V., Vats, S., Jain, M., Bhojak, J., & Kamal, R. (2007). Antimicrobial activity of bioactive metabolites isolated from selected medicinal plants. Asian Journal of Experimental Sciences, 21, 267–272.
12. Multanen, M. (2002). Effect of nitrate and ofloxacin blended caprolactone-l-lactide coatings on bioabsorbable self-reinforced polylactide urospirals properties (Doctoral dissertation). Tampere University, Finland.
13. Owais, M., Sharad, K. S., Shehbaz, A., & Saleemuddin, M. (2005). Antibacterial efficacy of *Withania somnifera* against experimental murine salmonellosis. Phytomedicine, 12(3), 229–235. Perumal, P., & Mahmud, R. (2013). Chemical analysis, inhibition of biofilm formation and biofilm eradication potential of plant extracts. BMC Complementary and Alternative Medicine, 13, 1–11.
14. Rebl, H., Renner, J., Kram, W., Springer, A., Fritsch, N., Hansmann, H., Hakenberg, O. W., & Nebe, J. B. (2020). Prevention of encrustation on ureteral stents: Which surface parameters provide guidance for the development of novel stent materials? Polymers, 12(3), 558.
15. Salman, R. A., Jameel, S. K., & Shakir, S. M. (2023). Study of antimicrobial activity of silver nanoparticles. Journal of Medicinal Chemistry Sciences, 6(4), 733–745.
16. Scotland, K. B., Lo, J., Grgic, T., & Lange, D. (2019). Ureteral stent-associated infection and sepsis: Pathogenesis and prevention. Biofouling, 35(1), 117–127.
17. Silva, T., Pokhrel, L. R., Dubey, B., Tolaymat, T. M., Maier, K. J., & Liu, X. (2009). Mechanisms of silver nanoparticle antimicrobial activity. Environmental Science & Technology, 43(12), 455–462.
18. Szell, T. F. F. D., Goelz, H., Bluemel, B., Heller, S., Stief, C. G., & Gratzke, C. (2019). In vitro effects of coating agents on bacterial biofilm development on ureteral stents. Journal of Endourology, 33(3), 225–231.
19. Vazquez-Munoz, R., Meza-Villezcas, A., Fournier, P. G. J., Soria-Castro, E., Juarez-Moreno, K., Gallego-Hernandez, A. L., & Huerta-Saquero, A. (2019). Enhancement of antibiotics antimicrobial activity due to silver nanoparticles. PLoS ONE, 14(11), e0224904.
20. Yaqoob, A. A., Umar, K., & Ibrahim, M. N. M. (2020). Silver nanoparticles: Various methods of synthesis, size affecting factors and their potential applications. Applied Nanoscience, 10, 1369–1378.
21. Zelichenko, G., Steinberg, D., Lorber, G., et al. (2013). Prevention of initial biofilm formation on ureteral stents. Journal of Endourology, 27(3), 333–337.